Longitudinal Monitoring of Flow-Diverting Stent Tissue Coverage After Implant in a Bifurcation Model Using Neurovascular High-Frequency Optical Coherence Tomography

Jildaz Caroff, MD, PhD [*‡]
Robert M. King, MS [*]
Giovanni J. Ughi, PhD [*]
Miklos Marosfoi, MD [*]
Erin T. Langan, BS [*]
Christopher Raskett, BS [*]
Ajit S. Puri, MD [*]
Matthew J. Gounis, PhD [*]

[*]Department of Radiology, New England Center for Stroke Research, University of Massachusetts Medical School, Worcester, Massachusetts; [‡]Department of Interventional Neuroradiology, NEURI Center, Bicêtre Hospital, Assistance Publique Hôpitaux de Paris, Le Kremlin-Bicêtre, France

This work has been presented in part of the SNIS Annual Meeting (poster), July 2019, Miami, Florida.

Correspondence:
Matthew J. Gounis, PhD,
Department of Radiology,
New England Center for Stroke Research,
University of Massachusetts,
55 Lake Ave N, SA-107R,
Worcester MA 01655, USA.
Email: matt.gounis@umassmed.edu

Received, October 30, 2019.
Accepted, March 19, 2020.
Published Online, May 28, 2020.

BACKGROUND: Tissue growth over covered branches is a leading cause of delayed thrombotic complications after flow-diverter stenting (FDS). Due to insufficient resolution, no imaging modality is clinically available to monitor this phenomenon.

OBJECTIVE: To evaluate high-frequency optical coherence tomography (HF-OCT), a novel intravascular imaging modality designed for the cerebrovascular anatomy with a resolution approaching 10 microns, to monitor tissue growth over FDS in an arterial bifurcation model.

METHODS: FDS were deployed in a rabbit model (n = 6), covering the aortic bifurcation. The animals were divided in different groups, receiving dual antiplatelet therapy (DAPT) (n = 4), aspirin only (n = 1), and no treatment (n = 1). HF-OCT data were obtained *in vivo* at 3 different time points in each animal. For each cross-sectional image, metal and tissue coverage of the jailed ostium was quantified. Scanning electron microscopy images of harvested arteries were subsequently obtained.

RESULTS: Good quality HF-OCT data sets were successfully acquired at implant and follow-up. A median value of 41 (range 21-55) cross-sectional images were analyzed per ostium for each time point. Between 0 and 30 d after implant, HF-OCT analysis showed a significantly higher ostium coverage when DAPT was not given. After 30 d, similar growth rates were found in the DAPT and in the aspirin group. At 60 d, a coverage of 90% was reached in all groups.

CONCLUSION: HF-OCT enables an accurate visualization of tissue growth over time on FDS struts. The use of FDS in bifurcation locations may induce a drastic reduction of the jailed-branch ostium area.

KEY WORDS: Intracranial aneurysm, Flow diverter, Optical coherence tomography, Endothelialization

Neurosurgery 87:1311–1319, 2020 DOI:10.1093/neuros/nyaa208 www.neurosurgery-online.com

Flow diversion represents a paradigm shift for the endovascular treatment of intracranial aneurysms. In large carotid siphon aneurysm indications, the long-term flow diverting stents (FDS) results have proven to be excellent[1]; their use in small,[2] distal,[3] and bifurcation aneurysms is increasingly reported.[4] However, the use of FDS in bifurcation aneurysms is controversial, and high rates of ischemic complications have been reported in the jailed territory.[4-8]

ABBREVIATIONS: DSA, digital subtraction angiography; **DAPT,** dual antiplatelet therapy; **FDS,** flow diverting stents; **HF-OCT,** high-frequency optical coherence tomography; **OSCR,** ostium surface coverage ratio; **PED,** pipeline embolization device; **SEM,** scanning electron microscopy; **2D,** 2-dimensional

Despite an increased usage, their healing mechanism is only partially understood. It is thought to be a continuous endothelialization of the device struts, in combination with a progressive aneurysm thrombosis.[9] However, neointima formation over jailed branches can be harmful, causing delayed ischemic complications following treatment.[10]

Although associated with hemorrhagic complications, dual antiplatelet therapy (DAPT) is required to prevent FDS thrombosis and it

is considered mandatory.[11] Nevertheless, the existing antiplatelet protocols are highly heterogeneous among different centers, with treatment durations that may vary from 3 mo to life-long. Existing imaging tools allow the monitoring of an excessive neointimal reaction,[12] however, due to insufficient spatial resolution, conventional x-ray based systems do not allow the evaluation of the device endothelialization process.

Intravascular imaging techniques have been extensively adopted for the investigation of peripheral and coronary arteries,[13] but existing devices are unsuitable for use in tortuous neurovasculature.[14] High-frequency optical coherence tomography (HF-OCT) is a novel modality designed for intravascular use in the cerebrovascular anatomy. With a spatial resolution approaching 10 microns, HF-OCT allows the user to visualize fine details about the interaction between the endovascular devices and the arterial wall, unprecedented in the field of neurovascular imaging.[15,16] In this study, we sought to evaluate the use of HF-OCT to monitor tissue growth over FDS in an arterial bifurcation rabbit model.

METHODS

The Institutional Animal Care and Use Committee (IACUC) approved all animal research activities. Six New Zealand White rabbits (n = 6; sex: either, weight range 3.0-4.0 kg) were included in this study.

Antiplatelet Regimen

Four animals (n = 4) were premedicated with a standard of care DAPT regimen consisting of oral administration of aspirin (10 mg/kg/d) and clopidogrel (10 mg/kg/d), beginning at least 5 d prior to implant, and continued for the duration of the study.[17] Two animals were used as controls: one was given only aspirin (10 mg/kg/d), and the other one did not receive any antiplatelet therapy.

FDS Implant

All procedures were performed under general anesthesia using a strict aseptic technique. Prior to all surgical procedures, the animals were pre-anesthetized by a subcuticular injection of atropine (0.01 mg/kg) and given an intramuscular dose of sustained-release buprenorphine (0.03 mg/kg) for pain management. Anesthesia was induced by an intramuscular injection of ketamine (35 mg/kg) and xylazine (5 mg/kg) and maintained with mechanical ventilation of 1% to 3% isoflurane. The physiologic status of the animal was assessed using continuous monitoring of respiration rate, heart rate, oxygen saturation level, end-tidal CO_2 level, and temperature.

Once anesthetized, the right femoral artery was exposed through a 2 cm incision. A 6-French introducer sheath was inserted over a guidewire and through an arteriotomy of the femoral artery. A Navien-072 guide catheter (Medtronic Neurovascular; Medtronic, Dublin, Ireland) was positioned in the right iliac artery. A pipeline embolization device (PED) (Medtronic Neurovascular) was deployed without any compression and in a way that its center was covering the aortic bifurcation (Figure 1). PED length was 20 mm and diameter chosen in a 3.25 to 3.75 mm range based on digital subtraction angiography (DSA) measurements. After implant, DSA and HF-OCT acquisitions were performed, then the femoral artery was ligated.

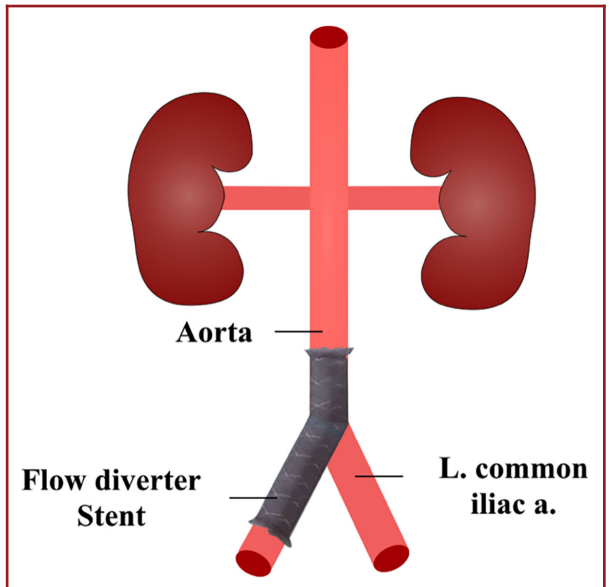

FIGURE 1. *Schematic representation of the abdominal aorta and aortic bifurcation. The FDS was inserted from the right femoral artery in order to cover the aortic bifurcation. L common iliac a - left common iliac artery.*

Follow-up Imaging

Under the same conditions of the FDS implant, 2 different imaging procedures were performed for the 2 different follow-up time points. For the first procedure, the left carotid artery was exposed through a 2 cm incision. A 6-French introducer sheath was subsequently inserted over a guidewire and through an arteriotomy of the carotid artery. A Navien-072 catheter was then positioned at the level of the proximal end of the FDS and used to perform HF-OCT and DSA studies. For the second follow-up imaging procedure, this technique was repeated through the right cervical carotid artery.

HF-OCT Imaging Technique

HF-OCT data sets were acquired at the time of the implant, at 14 d, and at 60 d for all control animals (n = 2) and for a first group of the DAPT animals (n = 2). The remaining animals receiving DAPT (n = 2) underwent HF-OCT imaging at implant, at 6 d, and at 27 d. Imaging time points were chosen as follows: 14 d because it is known to be the peak for smooth muscle cell proliferation[18]; 30 d because it is known to be the peak for intimal hyperplasia[18]; 60 d in order to obtain a late evaluation, as tissue growth is usually slower on covered branches.

To acquire the HF-OCT data sets, an intravascular imaging prototype (Vis-M™, Gentuity LLC, Sudbury, Massachusetts) was navigated distally through the flow-diverter under fluoroscopy guidance. To displace the blood from the arterial lumen, iodine contrast (Omnipaque 240; GE Healthcare, Marlborough, Massachusetts) was injected at a continuous rate of 4 mL/s for approximately 4 to 5 s through the Navien-072. During the contrast injection, the Vis-M device was automatically retracted at a constant speed, and the HF-OCT data acquired. The HF-OCT system processes the data in real time, the images are displayed live during the pullback, and are immediately available for review.

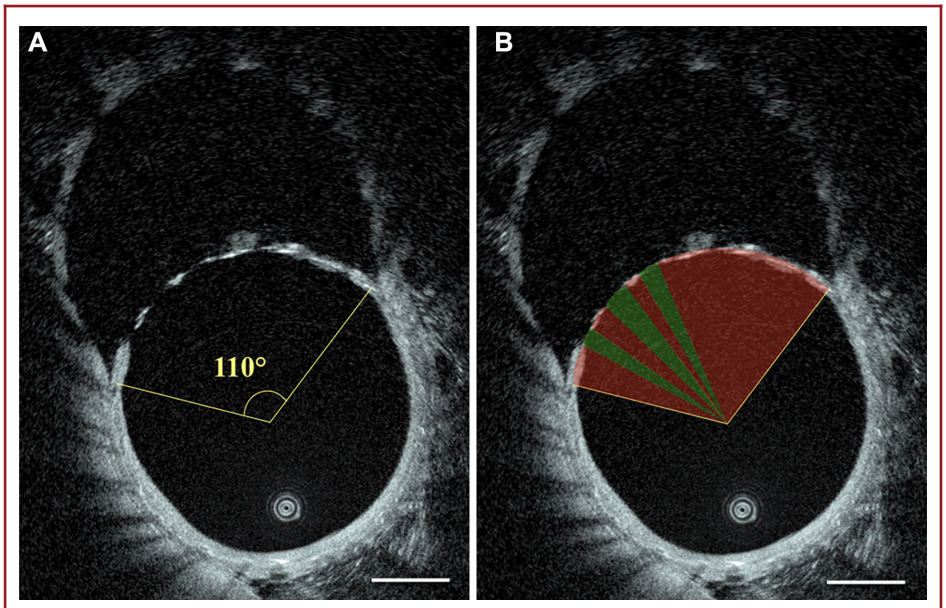

FIGURE 2. *Segmentation of the FDS covered segments.* **A**, *measurement of the ostium opening angle;* **B**, *determination of the OSCR. This procedure was repeated for all the HF-OCT cross-sections acquired over the bifurcation ostium and averaged for each follow-up study (ie, 3 different time points). Red area demarcates the tissue covered area of the device, and green where there remain open spaces. Scale bars are 1 mm.*

HF-OCT Data Analysis

HF-OCT data were processed to quantify the percentage of the ostial surface covered by metal and tissue by the means of software ImageJ (National Institutes of Health, Bethesda, Maryland). Three-dimensional data analysis was achieved by performing a sequential analysis of stacked 2-dimensional (2D) cross-sectional images. Specifically, the center of gravity of the vessel lumen was determined for each of the HF-OCT 2D images, and the full extension of the ostium was quantified using an angular measurement (Figure 2A). Subsequently, the covered and open fractions of the ostium angle were identified (Figure 2B). The extension of the coverage was quantified (%) for each section, as the ratio between the sum of covered angles (by tissue and/or struts) and the opening angle of the covered branch. This procedure was repeated for all the HF-OCT cross sectional images acquired over the left iliac artery ostium. The average of all 2D measurements was calculated to determine the 'ostium surface coverage ratio' (OSCR) and quantify the volumetric percentage of covered ostium for each animal at each different time points.

Scanning Electron Microscopy

After the final follow-up imaging procedure, the animal was euthanized and perfused with saline, followed by a 4% paraformaldehyde solution. After overnight immersion fixation in a 2.5% glutaraldehyde solution, the explants were rinsed in 0.1 M cacodylate buffer. The FDS were longitudinally cut under a dissecting microscope to expose the aortic bifurcation, and then dehydrated through a graded series of ethanol with concentrations up to 100%, followed by critical point drying in carbon dioxide. The samples were mounted on aluminum stubs, grounded with silver conductive paste, sputter coated with gold/palladium, and imaged using a FEI Quanta 200 MKII FEG SEM (Figure 3).

Statistical Analysis

Statistical analysis was performed using Prism software version 8.1 (GraphPad, San Diego, California). A normality test was applied to assess the Gaussian distribution of data in all cases. Results are shown as mean ± SD deviation. The medians of 2 independent groups, if non-normal distributions, were analyzed using the Mann–Whitney *U* test. Correlations were determined using Spearman correlation coefficients and *P*-values were considered significant if $< .05$.

RESULTS

DSA Analysis

For all the animals treated with at least one antiplatelet medication, DSA imaging did not reveal any occlusion of the jailed branch. The development of collateral circulation was not observed in any of the cases (n = 6).

In the control animal without any antiplatelet therapy (n = 1), DSA at day 14 showed slow filling of a narrowed jailed branch and vessel occlusion. In this case, the ostium coverage ratio was quantified to be equal to 98% (Figure 4) and the animal was subsequently sacrificed as it reached one of the study endpoints.

Percentage of Bifurcation Coverage as a Function of Time

Good quality HF-OCT data sets were successfully acquired in all cases. Approximately 41 OCT cross-sectional images were

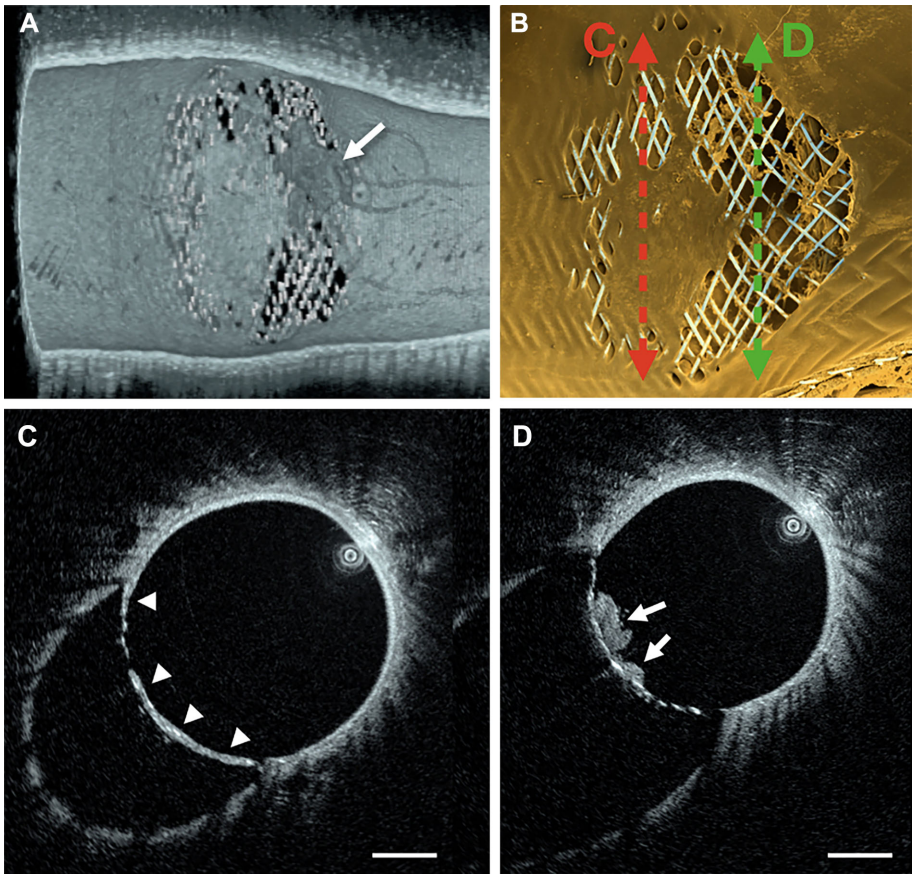

FIGURE 3. *Imaging at 27 d follow-up.* **A**, *Three-dimensional HF-OCT data rendering provides fine volumetric detail of the tissue covering the ostium of the iliac artery in vivo.* **B**, *ex vivo SEM imaging shows a high-degree of correlation with the HF-OCT findings. The arrow in panel* **A** *indicates the presence of a thrombus (having a darker appearance than the surrounding tissue) covering a portion of the jailed ostium, that is no longer visible after harvest and processing of the specimen for ex vivo imaging with SEM.* **C**, *high-resolution detail of the tissue covering the ostium of the aortic bifurcation (arrowheads).* **D**, *HF-OCT cross-sectional imaging showing micron-resolution detail of the clot over the flow-diverter struts (arrows). Scale bars are 1 mm.*

analyzed per ostium for each time point (median value equal to 41, with a range between 21 and 55).

Due to a risk of contrast overload, HF-OCT was not performed at the time of the implant in 2 animals. Given that the ostium coverage at baseline is only due to metallic struts, the missing baseline values were approximated in Figure 5 by averaging the OSCR values from the HF-OCT datasets acquired in the other 4 animals. This procedure resulted in an average post implant OSCR equal to 39% (range = 36%-41%).

In the DAPT group, the OSCR was quantified to be 62% at day 6 (n = 2), 67% at day 13 (n = 2), 85% at day 27 (n = 2), and 90% at day 60 (n = 2) (Figures 4 and 5). In the aspirin-only control animal, the OSCR was found to be equal to 81% at day 14 (n = 1), and 91% at day 60 (n = 1). For the animal that did not receive any antiplatelet therapy, the OSCR was 98% at day 14 (n = 1). Compared with the DAPT group, the ostium coverage was significantly higher at day 14 (+/− 1) in the aspirin group ($P < .0001$) but not at day 60 (Figure 5).

To analyze the antiplatelet effect on stent coverage, we measured the FDS coverage for each HF-OCT cross-section over the ostium and performed a comparison between all images from the aspirin and those from the DAPT regimen groups. At 14 d (±1), we found a mean ostium slice coverage ratio of 81% and 67% for the aspirin (over a total of n = 31 sections) and the DAPT groups (n = 75 sections), respectively ($P < .0001$). At 60 d, no difference was found ($P = .2$), with a mean OSCR of 91% for the aspirin group (n = 41 sections), and 90% for the DAPT group (n = 104 sections).

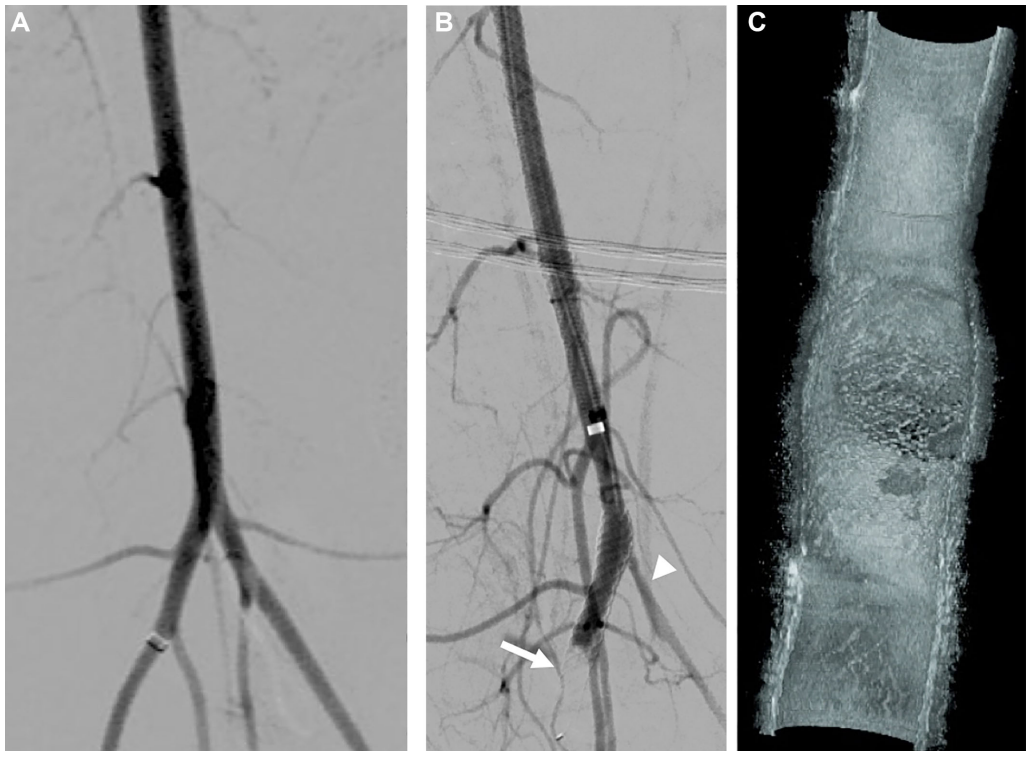

FIGURE 4. *Control animal without antiplatelet medication.* **A**, *DSA after implant shows a normal flow in the jailed left iliac branch.* **B**, *after 14 d, DSA shows a caliber reduction of the left iliac artery (arrowhead), associated with an impaired flow and the occlusion of the distal end of the FDS (arrow).* **C**, *Three-dimensional HF-OCT data rendering depicting an almost complete occlusion of the jailed ostium (98% OSCR) and presence of clots.*

Endothelialization Patterns

For each 2D cross-section, the OSCR was correlated with the location of the cross-section within the ostium (center vs periphery). For cross-sections closer to the center (Figure 6), the ostium shows a wide angle. In the periphery, the ostium shows a narrower angle. In the DAPT group, a significant peripheral coverage dominance at day 13 was found (Spearman $r = -0.41$, $P < .0002$) (Figure 7) meaning that after implant the neointima formation follows a centripetal pattern. This dominance was no longer observed after 13 d.

DISCUSSION

FDS use in Bifurcation Aneurysms

Although the use of FDS in bifurcation cases is increasingly reported,[8] the safety and efficacy of these procedures are still controversial. A recent meta-analysis showed a non-negligible rate of treatment-related complications (20%), suggesting that FDS in bifurcation should only be considered as an alternative treatment when conventional treatment methods are unfeasible.[8] In this analysis, the overall rate of flow impairment in the jailed branch (defined as a diminished flow or an artery occlusion) was 36%, with a 5.3% related incidence of symptoms.

It has been suggested that immediate ischemic complications are often related to flow diversion in the covered branch. These complications can be prevented with an optimal antiplatelet regimen, accurate blood pressure management, and using GP IIb/IIIa inhibitors.[19]

Delayed complications, however, have been related to progressive endothelialization leading to a drastic narrowing of the jailed ostium.[8] In this study, the ostial tissue-free surface was observed to be only 10% of the original area after 2 mo. Notably, since the tissue growth along the surface of the flow diverter is below the resolution DSA, stenosis is not depicted and vessels appear patent on DSA.

In a study by Shapiro et al,[19] at the time of the implant, a metal coverage ratio up to 30% (for jailed bifurcation branches) was found. The authors reported that this coverage ratio is expected to be well-tolerated regardless of the device size, the artery diameter, or the availability of immediate collateral support. They also demonstrated that when an OSCR of 90% is reached, the flow going through the FDS is only 15% or less of its initial value. Thus, for cases with insufficient collateral circulation, the

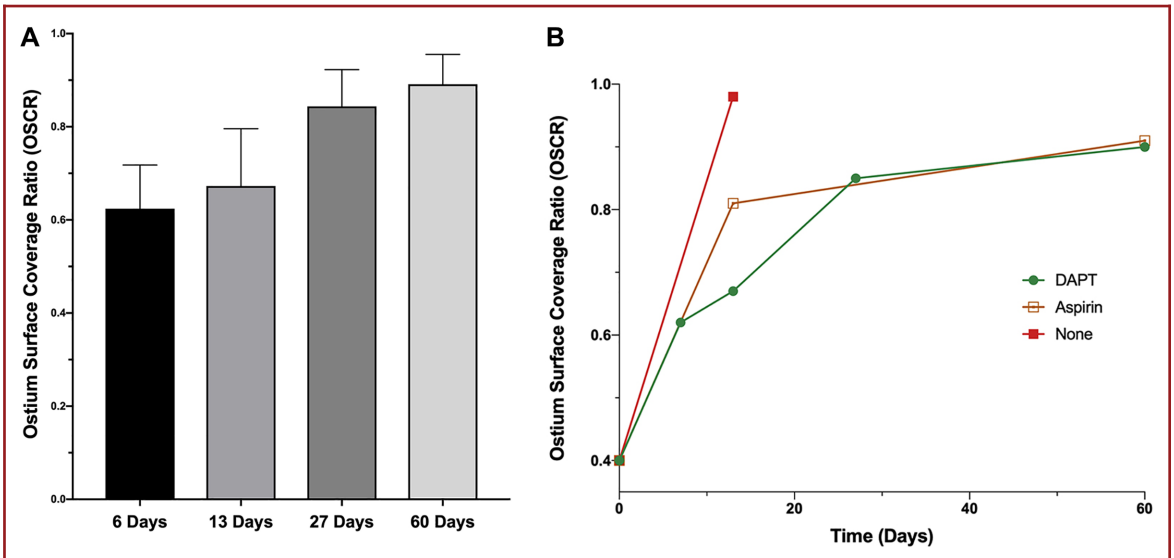

FIGURE 5. **A**, *OSCR as a function of time in the DAPT group.* **B**, *OSCR as a function of time for the 3 different groups.*

progressive endothelialization and the subsequent flow reduction can put the patient at risk for a delayed ischemic lesion.

New Zealand White Rabbit Bifurcation Model

In a swine bifurcation model, Iosif et al[20] have reported similar rates of ostial coverage between 81% and 98%. However, in this model, the vascular territory supplied by the ascending pharyngeal artery presents an extensive collateral supply. It is possible to theorize that the presence of such extensive collaterals might have caused the elevated coverage ratio observed at 3 mo.

Our study corroborated those results using a high-flow, terminal artery, jailed by the device trying to reproduce the normal response of human intracranial bifurcations. The development of this model was uniquely possible using the reduced profile of the imaging probe provided with the HF-OCT system, as compared with conventional OCT solutions designed for use in the coronaries.[21]

HF-OCT Monitoring of Jailed Ostia

HF-OCT allowed detailed longitudinal monitoring of the tissue coverage over the jailed ostia. We have observed that DAPT induces a slower coverage formation over the stent struts. This finding reinforces the idea that an efficient antiplatelet therapy is required not only in acute settings but also for months following when treating arterial bifurcations with FDS. It is possible to speculate that a slower coverage formation might allow collateral pathways to fully develop and balance the flow reduction related to a high OSCR.

In the control group without antiplatelet medication, DSA at day 14 demonstrated slow filling and reduced caliber of the jailed iliac artery. HF-OCT showed a very high ostium coverage ratio. This rabbit model, in combination with HF-OCT, can be used in the near future to evaluate the new coated FDS (developed for providing lower thrombogenicity) without antiplatelet medication.[22] Furthermore, a high correlation with scanning electron microscopy (SEM) demonstrated that HF-OCT can accurately depict the tissue coverage morphology and micro-structure, differentiating between 2 different patterns. One is a thin, irregular and mostly interstruts coverage possibly corresponding to a scaffold of inflammatory and smooth-muscle cells.[23] The second pattern is a thick and more regular coverage, likely to correspond to neo-intima formation as illustrated by SEM (Figure 8).

Pathophysiology

Based on the coverage distribution observed over the ostium, we have found a statistically significant, peripheral predominance that can be observed after day 13, but at no other time point. After implant, early stage coverage largely consists of inflammatory cell layers[9] that may arise from the circulation and possibly explaining the homogeneous coverage distribution observed at day 6.

In rabbit models, the smooth muscle cell proliferation is known to peak at day 14.[18,24] However, the origin of the endothelial cells covering the FDS still remains controversial. They are either believed to migrate from the adjacent parent artery or to arise from differentiation of circulating bone marrow-derived endothelial progenitor cells. Recent studies are suggesting that it is likely a result of both mechanisms.[25] No definitive conclusion can be drawn from the findings presented by this study, but the peripheral distribution we observed at day 13 could be related to a dominance of the contiguous mechanism in the early phase. If this trend is confirmed, it could reinforce the idea that the correct

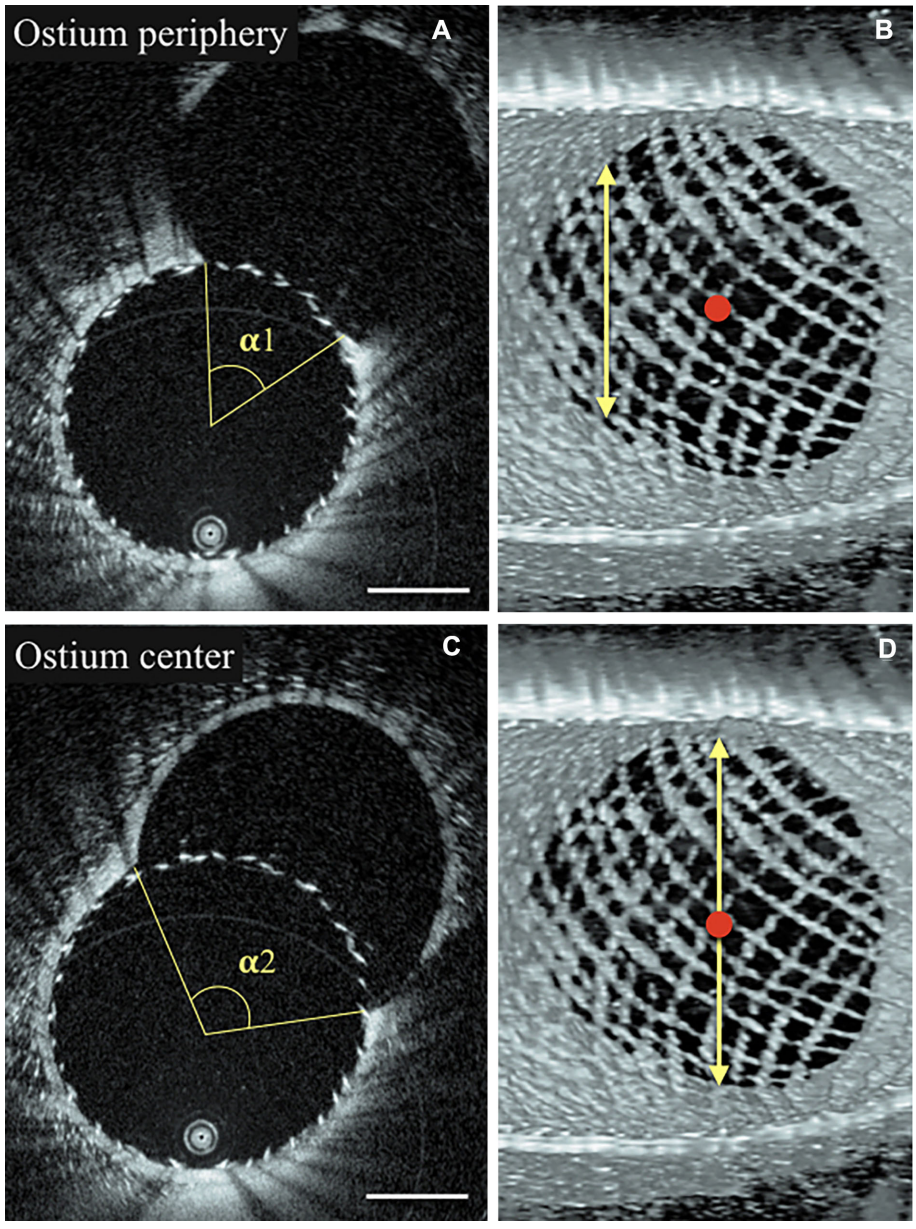

FIGURE 6. *The closer the 2D section is to the ostium center (red dot) the wider the opening angle of the ostium is.* **A**, *peripheral 2D HF-OCT section with a narrow opening angle.* **B**, *Corresponding 3-dimensional HF-OCT rendering, illustrating the section location on the proximal border of the ostium.* **C** *and* **D**, *images of a central section with a large opening angle. Scale bars represent 1 mm.*

apposition of FDS to the arterial wall is a key parameter for the healing of aneurysms,[26,27] as it would facilitate the migration of cells. This finding may support the future concept of performing a careful analysis of wall apposition by the means of a high-resolution imaging modality, and advocates for the use technical solutions where indicated (eg, balloon angioplasty).

HF-OCT for Personalized Care

Antiplatelet therapy is known to be a frequent source of both minor and major patient complications.[28] Despite the widespread use of FDS, no consensus can be found on optimal antiplatelet management. In some clinical centers, DAPT is often prescribed

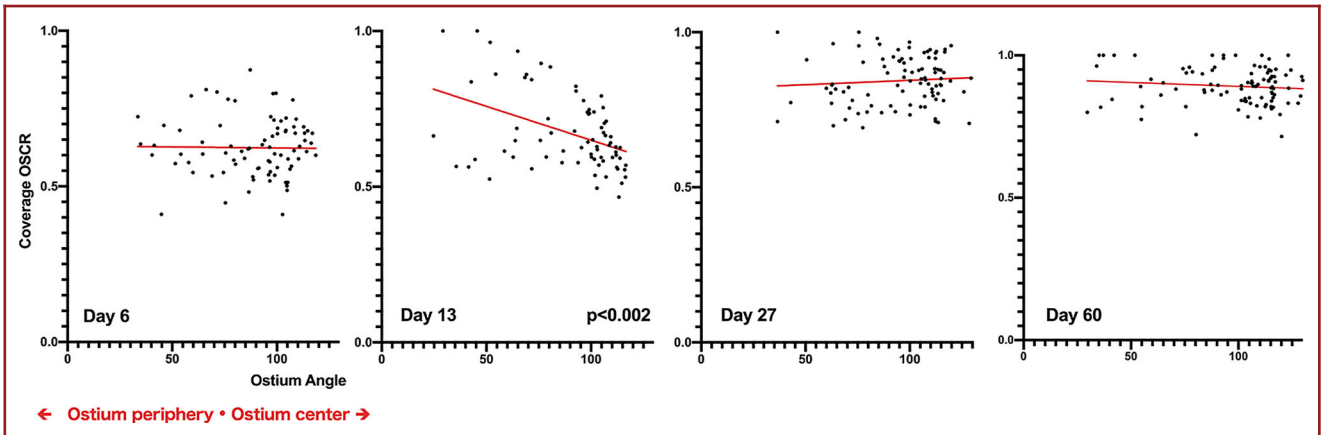

FIGURE 7. *Correlation between the coverage values and the location of the HF-OCT images (ie, their proximity to the isocenter or to the periphery of the ostium). The data scatter plot shows the OSCR value on the vertical y-axis vs the location of the cross-section (horizontal x-axis). The wider the ostium opening angle is (x-axis), the closer it is to the isocenter of the ostium. Each plot corresponds to a unique HF-OCT cross-sectional image from animals in the DAPT group. Data collected at day 13 show a statistically significant peripheral predominance of the OSCR.*

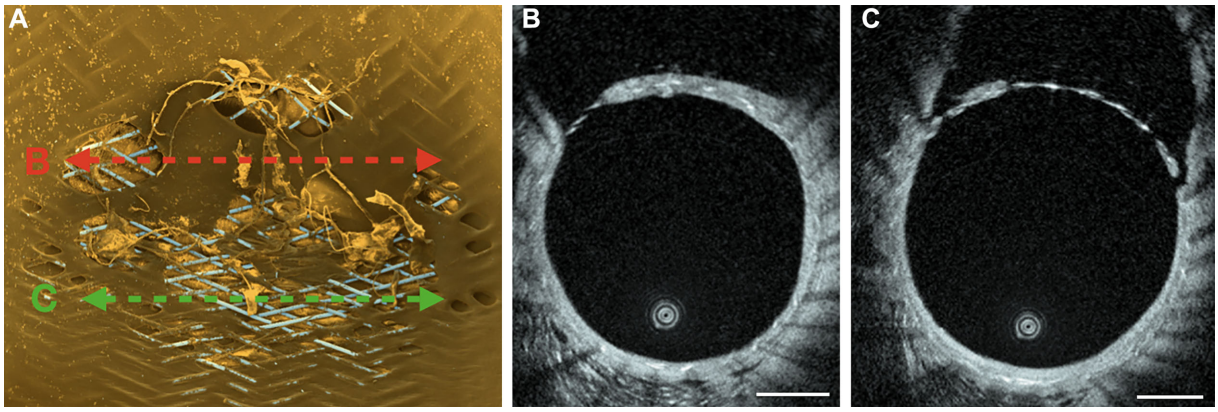

FIGURE 8. **A**, *At the level of a fully endothelialized section on SEM (red line),* **B**, *HF-OCT shows a thick and homogeneous FDS coverage.* **C**, *a thin irregular FDS coverage can be seen on HF-OCT, corresponding to a partial, non-endothelial cell coverage on SEM (***A***, green line). Scale bars indicate 1 mm.*

for no more than 3 mo and aspirin is prescribed for 1 yr[11]; other centers may prescribe DAPT for a period of 6 mo, followed by aspirin indefinitely.[29] In the near future, it is possible to imagine that optimal antiplatelet therapy can be modulated through an informed decision based on high-resolution imaging data, and that HF-OCT evidence of complete FDS endothelialization may allow the discontinuation of this medication.

Limitations

This study is limited by the small sample size. However, due to the very high resolution of HF-OCT, it was possible to quantify the ostium coverage in a large number of individual cross-sections in both the DAPT group (n = 355), and in the non-DAPT group (n = 93), allowing for a statistical comparison. Furthermore, although limited by potential differences between the human and rabbit biology, the results presented in this manuscript suggest a promising role for HF-OCT in the field of neuroendovascular surgery.

CONCLUSION

HF-OCT enables accurate visualization and quantification of tissue growth over FDS struts at the orifice of jailed arteries as a function of time. The use of FDS in bifurcation locations may induce a drastic reduction of the jailed-branch ostium area. In the near future, HF-OCT could potentially contribute to personalized care, helping the physician to determine the ideal antiplatelet regimen for each patient.

Disclosures

This research was partially supported by the US National Institute of Health (contracts R43 NS100163, and R44 NS100163) and by Gentuity LLC. Dr Caroff was supported by research grants from the Fulbright Program, the Philippe Foundation and the French society of radiology (SFR-CERF), and has received educational scholarships from Medtronic neurovascular and Microvention/Terumo. Dr Ughi is an employee of Gentuity LLC and holds stock. Dr Marosfoi receives fees for service consulting for Stryker Neurovascular and Inneuroco Inc. Dr Gounis has received research support from the National Institutes of Health (NIH), the United States—-Israel Binational Science Foundation, Anaconda, Apic Bio, Arsenal Medical, Axovant, Cerenovus, Ceretrieve, Cook Medical, Galaxy LLC, Gentuity, Imperative Care, InNeuroCo, Insera, Magneto, Microvention, Medtronic Neurovascular, MIVI Neurosciences, Neuravi, Neurogami, Philips Healthcare, Progressive Neuro, Rapid Medical, Route 92 Medical, Stryker Neurovascular, Syntheon, and the Wyss Institute; is a consultant on a fee-per-hour basis for Cerenovus, Imperative Care, Medtronic Neurovascular, Mivi Neurosciences, Phenox, Route 92 Medical, and Stryker Neurovascular; and holds stock in Imperative Care, InNeuroCo and Neurogami.

REFERENCES

1. Becske T, Brinjikji W, Potts MB, et al. Long-Term clinical and angiographic outcomes following pipeline embolization device treatment of complex internal carotid artery aneurysms: five-year results of the pipeline for uncoilable or failed aneurysms trial. *Neurosurgery*. 2017;80(1):40-48.
2. Chalouhi N, Starke RM, Yang S, et al. Extending the indications of flow diversion to small, unruptured, saccular aneurysms of the anterior circulation. *Stroke*. 2014;45(1):54-58.
3. Cagnazzo F, Perrini P, Dargazanli C, et al. Treatment of unruptured distal anterior circulation aneurysms with flow-diverter stents: a meta-analysis. *AJNR Am J Neuroradiol*. 2019;40(4):687-693.
4. Caroff J, Neki H, Mihalea C, et al. Flow-Diverter stents for the treatment of saccular middle cerebral artery bifurcation aneurysms. *AJNR Am J Neuroradiol*. 2016;37(2):279-284.
5. Saleme S, Iosif C, Ponomarjova S, et al. Flow-Diverting stents for intracranial bifurcation aneurysm treatment. *Neurosurgery*. 2014;75(6):623-631.
6. Iosif C, Camilleri Y, Saleme S, et al. Diffusion-weighted imaging–detected ischemic lesions associated with flow-diverting stents in intracranial aneurysms: safety, potential mechanisms, clinical outcome, and concerns. *J Neurosurg*. 2015;122(3):627-636.
7. Michelozzi C, Darcourt J, Guenego A, et al. Flow diversion treatment of complex bifurcation aneurysms beyond the circle of willis: complications, aneurysm sac occlusion, reabsorption, recurrence, and jailed branch modification at follow-up. *J Neurosurg*. 2018;131(6):1751-1762.
8. Cagnazzo F, Mantilla D, Lefevre PH, Dargazanli C, Gascou G, Costalat V. Treatment of middle cerebral artery aneurysms with flow-diverter stents: a systematic review and meta-analysis. *AJNR Am J Neuroradiol*. 2017;38(12):2289-2294.
9. Kadirvel R, Ding Y-H, Dai D, Rezek I, Lewis DA, Kallmes DF. Cellular mechanisms of aneurysm occlusion after treatment with a flow diverter. *Radiology* 2014;270(2):394-399.
10. Zhou G, Su M, Yin Y-L, Li M-H. Complications associated with the use of flow-diverting devices for cerebral aneurysms: a systematic review and meta-analysis. *Neurosurg Focus*. 2017;42(6):E17.
11. Narata AP, Amelot A, Bibi R, et al. Dual antiplatelet therapy combining aspirin and ticagrelor for intracranial stenting procedures: a retrospective single center study of 154 consecutive patients with unruptured aneurysms. *Neurosurgery*. 2018;84(1):1360.
12. Caroff J, Iacobucci M, Rouchaud A, et al. The occurrence of neointimal hyperplasia after flow-diverter implantation is associated with cardiovascular risks factors and the stent design. *J NeuroInterv Surg*. 2018;11(6):610-613.
13. Tearney GJ, Regar E, Akasaka T, et al. Consensus standards for acquisition, measurement, and reporting of intravascular optical coherence tomography studies. *J Am Coll Cardiol*. 2012;59(12):1058-1072.
14. Chen CJ, Kumar JS, Chen SH, et al. Optical coherence tomography. *Stroke*. 2018;49(4):1044-1050.
15. Gounis MJ, Ughi GJ, Marősfoi M, et al. Intravascular optical coherence tomography for neurointerventional surgery. *Stroke*. 2019;50(1): 218-223.
16. King RM, Marősfoi M, Caroff J, et al. High frequency optical coherence tomography assessment of homogenous neck coverage by intrasaccular devices predicts successful aneurysm occlusion. *J Neurointerv Surg*. 2019;11(11):1150-1154.
17. Dai D, Ding YH, Kadirvel R, Rad AE, Lewis DA, Kallmes DF. Patency of branches after coverage with multiple telescoping flow-diverter devices: an in vivo study in rabbits. *AJNR Am J Neuroradiol*. 2012;33(1):171-174.
18. More RS, Rutty G, Underwood MJ, Brack MJ, Gershlick AH. A time sequence of vessel wall changes in an experimental model of angioplasty. *J. Pathol*. 1994;172(3):287-292.
19. Shapiro M, Shapiro A, Raz E, Becske T, Riina H, Nelson PK. Toward better understanding of flow diversion in bifurcation aneurysms. *AJNR Am J Neuroradiol*. 2018;39(12):2278-2283.
20. Iosif C, Ponsonnard S, Roussie A, et al. Jailed artery ostia modifications after flow-diverting stent deployment at arterial bifurcations. *Neurosurgery*. 2016;79(3):473-480.
21. Ughi GJ, Wang H, Gerbaud E, et al. Clinical characterization of coronary atherosclerosis with dual-modality OCT and near-infrared autofluorescence imaging. *JACC Cardiovasc Imaging*. 2016;9(11):1304-1314.
22. Caroff J, Tamura T, King RM, et al. Phosphorylcholine surface modified flow diverter associated with reduced intimal hyperplasia. *J NeuroIntervent Surg* 2018;10(11):1097-1101.
23. Malle C, Tada T, Steigerwald K, et al. Tissue characterization after drug-eluting stent implantation using optical coherence tomography. *Arterioscler Thromb Vasc Biol*. 2013;33(6):1376-1383.
24. Curcio A, Torella D, Indolfi C. Mechanisms of smooth muscle cell proliferation and endothelial regeneration after vascular injury and stenting: approach to therapy. *Circ J*. 2011;75(6):1287-1296.
25. Ravindran K, Salem MM, Alturki AY, Thomas AJ, Ogilvy CS, Moore JM. Endothelialization following flow diversion for intracranial aneurysms: a systematic review. *AJNR Am J Neuroradiol*. 2019;40(2):295-301.
26. Rouchaud A, Ramana C, Brinjikji W, et al. Wall apposition is a key factor for aneurysm occlusion after flow diversion: a histologic evaluation in 41 rabbits. *AJNR Am J Neuroradiol*. 2016;37(11):1-5.
27. King RM, Brooks OW, Langan ET, et al. Communicating malapposition of flow diverters assessed with optical coherence tomography correlates with delayed aneurysm occlusion. *J NeuroInterv Surg*. 2017;10(7):693-697.
28. Easton JD, Aunes M, Albers GW, et al. Risk for major bleeding in patients receiving ticagrelor compared with aspirin after transient ischemic attack or acute ischemic stroke in the SOCRATES study (Acute stroke or transient ischemic attack treated with aspirin or ticagrelor and patient outcomes). *Circulation*. 2017;136(10):907-916.
29. Jabbour P, Chalouhi N, Tjoumakaris S, et al. The pipeline embolization device: learning curve and predictors of complications and aneurysm obliteration. *Neurosurgery*. 2013;73(1):113-120; discussion 120.